TN 1179

NATIONAL ADVISORY COMMITTEE FOR AERONAUTICS

TECHNICAL NOTE

No. 1179

NOTES ON THE THEORETICAL CHARACTERISTICS OF TWO-DIMENSIONAL SUPERSONIC AIRFOILS

By H. Reese Ivey

Langley Memorial Aeronautical Laboratory
Langley Field, Va.

Washington
January 1947

NACA LIBRARY
LANGLEY MEMORIAL AERONAUTICAL LABORATORY
Langley Field, Va.

NASA Technical Library
3 1176 01425 7522

NATIONAL ADVISORY COMMITTEE FOR AERONAUTICS

TECHNICAL NOTE NO. 1179

NOTES ON THE THEORETICAL CHARACTERISTICS OF TWO-DIMENSIONAL SUPERSONIC AIRFOILS

By H. Reese Ivey

SUMMARY

The shock-expansion method of NACA TN No. 1143 was used to determine the principal aerodynamic characteristics of two-dimensional supersonic airfoils. A discussion is given of the effect of thickness ratio, free-stream Mach number, angle of attack, camber, thickness distribution, and aileron deflection. The calculations indicated that the minimum drag of supersonic airfoils is obtained when the maximum thickness is behind the 0.50 chord. The center of pressure obtained for a symmetrical supersonic airfoil was found to be ahead of the 0.50 chord.

INTRODUCTION

The characteristics of thin airfoils moving at supersonic speeds are determined in reference 1 by Ackeret's thin-airfoil theory. In this method, the local static pressure is assumed to vary linearly with the angle between the free-stream direction and the local airfoil surface. This assumption precludes any effect of camber on lift and locates the center of pressure of an uncambered airfoil at the midchord.

The relations for flow across shock waves are presented in reference 2. Reference 3 combines these shock equations with Meyer's expansion equations (see reference 4) and presents a graphical way of calculating a second-order approximation to the characteristics of thin sharp-nose airfoils at supersonic speeds. The present paper uses the shock-expansion method of reference 3 to determine some interesting effects of thickness ratio, free-stream Mach number, angle of attack, camber, thickness distribution, and aileron deflection. Swept-back wings are not considered herein as they are of sufficient interest to justify a separate report.

SYMBOLS

M	Mach number
p	static pressure
q	dynamic pressure
α	angle of attack of airfoil
c_l	section lift coefficient
c_d	section drag coefficient
$c_{m_{.5c}}$	coefficient of section pitching moment about airfoil midchord
t	airfoil thickness
c	airfoil chord
c_a	aileron chord
δ	aileron deflection

Subscripts:

o	free stream
1	upper leading surface
2	upper trailing surface
3	lower leading surface
4	lower trailing surface
max	maximum

DISCUSSION

Airfoils experience an increased pressure drag at high Mach numbers. This drag increase can be minimized by the use of thin airfoils with sharp leading edges. For this reason, and also because theoretical calculations are more accurate

for this type of airfoil, the wing sections considered herein are limited to fairly thin, sharp-nose airfoils having little surface curvature.

Center of pressure.- Reference 3 has given the pressure distribution at $M_o = 4$ the diamond-shape (symmetric double-wedge) airfoil shown in figure 1. The pressure coefficients around this airfoil are given in, table I, as follows:

TABLE I.- PRESSURE COEFFICIENTS

Location of surface (see fig. 1)	Pressure coefficient, $\frac{p-p_o}{q_o}$
Upper leading	-0.0169
Lower leading	.0416
Upper trailing	-.0308
Lower trailing	.0188

A study of this table brings out many interesting points on the characteristics of supersonic airfoils. The lift of the airfoil is proportional to the difference in the pressure coefficients on the upper and lower surfaces of the airfoil. For the leading half of the airfoil of figure 1, this difference is

$$0.0416 + 0.0169 = 0.0585$$

For the trailing half of the airfoil the difference is

$$0.0308 + 0.0188 = 0.0496$$

The significant result to be noted is that the front of the airfoil is carrying more than half the lift and the center of pressure is found to be at the 46-percent-chord position. As the supersonic Mach number is decreased toward 1.0, the center of pressure of thin diamond-shape airfoils approaches the 50-percent-chord position. As the supersonic Mach number is increased, the center of pressure of thicker airfoils moves forward. Figure 2 shows the variation of the center of pressure of a 5-percent-thick diamond-shape airfoil with angle of attack and Mach number. The actual shift in center of pressure depends on the airfoil shape. For example, a wedge airfoil having its

maximum thickness at the trailing edge will have its center of pressure at midchord at all supersonic speeds provided that the angle of attack is not sufficient to cause the shock wave to separate from the leading edge.

Drag coefficient.- In order to determine the actual variation of drag, some allowance must be made for the viscous skin friction. Theoretical work (reference 2) suggests that the viscous drag coefficient decreases with increasing Reynolds number at supersonic speeds. However, reference 5 shows that the viscous drag coefficient is almost unaffected by changes in Mach number or Reynolds number if the Reynolds number is very high. For this reason the skin-friction drag coefficient based on wing area is considered herein to be constant at 0.0060, which is approximately the value obtained for recent highly polished jet-propelled fighters; however, the results are plotted in such a way that the reader can easily adjust the curves to correspond with the conditions in which he is interested. If new information indicates that the variation of friction with Mach number is appreciable, the curves may be raised or lowered by the amount of the variation.

Figure 3 shows the variation of the drag coefficient of diamond-shape airfoils with thickness ratio and free-stream Mach number. The graph shows that the drag coefficients are very high near a Mach number of 1.0 and the main part of the drag then is pressure drag. At high Mach numbers the shock drag has decreased in importance relative to skin friction. It is seen that the Ackeret method (reference 1) gives almost the same trends as the shock-expansion method except that it shows a less rapid variation of drag with thickness at high Mach numbers than the present shock-expansion method. Ackeret's method predicts lower pressure increases on the leading portion of the airfoil and higher pressure decreases on the trailing portion than the method of combining the shock and expansion relations.

The effect of the location of the maximum thickness on the drag coefficient for a 5-percent-thick airfoil is shown in figure 4. This figure indicates that the optimum location of maximum thickness is close to the midchord position for fairly low supersonic speeds. At Mach numbers of 8 and above, however, the optimum location seems to be near the trailing edge. This condition is very different from that predicted by Ackeret's method where, by the nature of his assumptions, the pressure distribution is symmetrical. In connection with airfoils designed for an angle of attack other than zero it must be kept

in mind that the optimum location of thickness on the upper and lower surfaces will be different.

Figure 5 shows the effect of location of maximum thickness on the drag of 10-percent-thick airfoils. These airfoils show an even greater variation from Ackeret's prediction than the 5-percent-thick airfoils. This figure indicates that the optimum position for maximum thickness at a Mach number of 8 is at the trailing edge. Actually, the flow at the trailing edge will break down for this condition and form a turbulent wake of somewhat higher pressure than that calculated. This breakdown of the theory for the airfoils with blunt trailing edges should make the experimental drag less than the theoretical drag for this extreme condition.

Lift coefficient.- In figure 6 the slope of the lift curve is plotted as a function of free-stream Mach number for three different airfoil thicknesses. At a Mach number slightly above 1 the slope of the lift curve is approximately equal to the subsonic slope. The slope of the lift curve drops rapidly, however, with increasing Mach number. The trend of the curve is similar to the drag curve of figure 3 except that the drag curve was displaced upward a constant amount by the skin friction. The thickness ratio of the airfoil seems to have little effect on the slope of the lift curve except at high supersonic Mach numbers (above 4). The thick sections then have the highest slope. As might be expected, the calculation obtained by the shock-expansion method for airfoils of zero thickness give results identical with those given by Ackeret's method.

Lift-drag ratio.- The effect of angle of attack and Mach number on the characteristics of a 5-percent-thick double-wedge airfoil is shown in figure 7. This figure shows that the lift coefficient increases almost linearly with angle of attack, and the drag coefficient increases with angle of attack in a manner similar to the variation of total drag coefficient for a complete subsonic wing.

The maximum lift-drag ratio c_l/c_d at a Mach number of 2 is approximately 6.92 at $c_l = 0.16$ and $\alpha = 4°$. At a Mach number of 4 the maximum ratio is 5.52 at $c_l = 0.094$ and $\alpha = 5°$. The maximum lift-drag ratio decreases with increasing Mach number, and the lift coefficient for maximum lift-drag ratio also decreases with increasing Mach number. These trends are somewhat different from those of reference 1 in which skin friction was neglected. In that case the maximum lift-drag ratio was independent of Mach number. Busemann in reference 6 calculates the Mach number at which the lift-drag ratio is maximum for certain airfoil thicknessos.

Camber.- Table I has shown that the leading portion of an airfoil tends to carry more than its share of the lift and, hence,

it can be expected that camber, which decreases the angle of attack of this important part of the airfoil, will decrease the lift. In figure 8, calculations show that the addition of 1.25 percent camber changes the characteristics given in figure 7 for Mach number 4. The addition of camber increases the drag coefficient at zero angle of attack but decreases the drag coefficient at high angle of attack. The angle of zero lift is shifted slightly but the slope of the lift curve remains essentially the same. It is significant that the shift obtained as a result of camber at supersonic speeds is opposite in direction to the shift obtained at subsonic speeds. This result indicates that a cambered wing will experience a change in the angle for zero lift in accelerating through the speed of sound. The addition of camber decreases the lift-drag ratio at low angles of attack and increases it at high angles of attack.

A comparison of the angle of attack for zero lift as calculated by the Ackeret method (reference 1), as calculated by the shock-expansion method of reference 3, and as determined experimentally by reference 7 is presented in table II. Thus,

TABLE II.- ANGLE OF ATTACK FOR ZERO LIFT AT MACH NUMBER 2.13

Airfoil shape	Angle of zero lift, deg		
	Ackeret theory (reference 1)	Shock-expansion method (reference 3)	Experimental (reference 7)
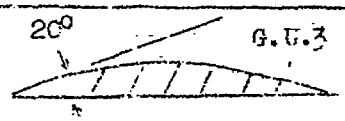	0	1.68	1.89
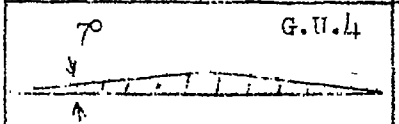	0	.44	.45
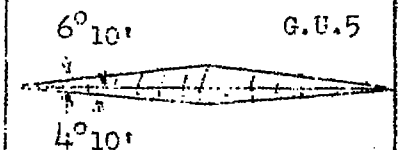	0	.28	.26

The shock-expansion method (reference 3) shows better agreement with experiment than the Ackeret method as far as the effect of camber is concerned. Theoretically, a slight error might be expected for the G.U.3 airfoil because of the interference of shock and expansion waves due to the continuous surface curvature; however, the error seems to be of very low magnitude.

In connection with table II it might be well to point out that higher order terms have been developed by other authors which, when added to the Ackeret theory, predict some effect of camber on lift.

Ailerons.- In order to demonstrate the effect of ailerons on supersonic airfoils, results are given in figure 9 to show the aileron effectiveness factor for a 5-percent-thick diamond-shape airfoil at a Mach number of 4 as a function of the ratio of aileron chord to airfoil chord. For comparison, a curve for the same airfoil is given for the subsonic (incompressible-flow) condition ($M = 0$), as well as one obtained by Ackeret's method. The aileron effectiveness factors $\frac{dc_l/d\delta}{dc_l/d\alpha}$ are shown to be much lower at supersonic speeds than at speeds where there are no compressibility effects. These values are also slightly lower than those obtained by the Ackeret method. For instance, a 20-percent-chord aileron at Mach number 4 has approximately the same effectiveness factor as a 1-percent-chord aileron at low subsonic speeds. This result indicates that the helix angle of an airplane in rolling will probably be much less at supersonic speeds than the helix angle described by airplanes at low subsonic speeds. At these speeds the aileron influences the wing ahead of it, but at supersonic speeds the aileron alone is affected. In fact, the wing at supersonic speeds leaves the aileron in low-density air, and thus the effectiveness is decreased to values lower than might otherwise be expected. The actual effectiveness varies for different airfoil shapes and thickness ratios. Figure 10 gives a curve of the variation of section lift coefficient due to aileron deflection and figure 11 gives the slope of this curve; a slight increase in aileron effectiveness with increasing deflection is indicated.

The section pitching-moment coefficient about the midchord $c_{m_{.5c}}$ as a function of aileron deflection δ is shown in figure 12. In figure 13 the slope of this curve $dc_{m_{.5c}}/d\delta$ is plotted against aileron deflection and shows an increased rate of change of pitching-moment coefficient with increasing aileron deflection. The pitching-moment coefficient about the midchord is plotted in figure 14 as a function of angle of attack for constant aileron deflection. The absolute value of the pitching-moment coefficient is shown to decrease with increasing angle of attack for a downward aileron deflection of 10° at $M = 4$.

CONCLUSIONS

Calculations made by the shock-expansion method to determine the aerodynamic characteristics of supersonic airfoils indicated the following conclusions:

1. Uncambered double-wedge airfoils having the maximum thickness at midchord will have their centers of pressure ahead of the 50-percent chord at high supersonic speeds, but this center of pressure will approach midchord as the Mach number is lowered toward 1.0. Airfoils having their maximum thickness near the trailing edge will have the center of pressure near the midchord at all supersonic speeds provided the angle of attack is not sufficient to cause the shock wave to separate from the leading edge.

2. The pressure-drag coefficient and the lift coefficient for the same angle of attack decrease in a similar manner with increasing Mach number, and thus their ratio is essentially constant with Mach number. The addition of a constant skin-friction drag coefficient results in a decrease in the lift-drag ratio with increasing Mach number.

3. The optimum location of maximum thickness for a given thickness ratio to give minimum drag depends on airfoil shape and free-stream Mach number. For double-wedge airfoils the optimum position of maximum thickness is near the trailing edge at very high Mach numbers; however, the optimum position approaches the midchord as the speed is decreased toward a Mach number of 1.0.

4. The aileron effectiveness factor is lower when estimated by the shock-expansion method than when estimated by the Ackeret method.

5. A comparison of theoretical and experimental values of the angle of zero lift suggests that the present method of calculation is a considerably closer approximation than Ackeret's method.

Langley Memorial Aeronautical Laboratory
National Advisory Committee for Aeronautics
Langley Field, Va., July 18, 1946

REFERENCES

1. Taylor, G. I.: Applications to Aeronautics of Ackeret's Theory of Aerofoils Moving at Speeds Greater Than That of Sound. R. & M. No. 1467, British A.R.C., 1932

2. von Kármán, Th.: The Problem of Resistance in Compressible Fluids. GALCIT Pub. No. 75, 1936. (From R. Accad. d'Italia, cl. sci. fis., mat. e nat., vol. XIV, 1936.)

3. Ivey, H. Reese, Stickle, George W., and Schuettler, Alberta: Charts for Determining the Characteristics of Sharp-Nose Airfoils in Two-Dimensional Flow at Supersonic Speeds. NACA TN No. 1143, 1946.

4. Taylor, G. I., and Maccoll, J. W.: The Mechanics of Compressible Fluids. Two-Dimensional Flow at Supersonic Speeds. Vol. III of Aerodynamic Theory, div. H, ch. IV, sec 2, W. F. Durand, ed., Julius Springer (Berlin), 1935, p. 238.

5. Theodorsen, Theodore, and Regier, Arthur: Experiments on Drag of Revolving Disk, Cylinders, and Streamline Rods at High Speeds. NACA ACR No. L4F16, 1944.

6. Busemann, A.: Aerodynamic Lift at Supersonic Speeds. 2844, Ae. Techl. 1201, British A.R.C., Feb. 3, 1937. (From Luftfahrtforschung, Bd. 12, Nr. 6, Oct. 3, 1935, pp. 210-220.)

7. Ferri, Antonio: Experimental Results with Airfoils Tested in the High-Speed Tunnel at Guidonia. NACA TM No. 946, 1940.

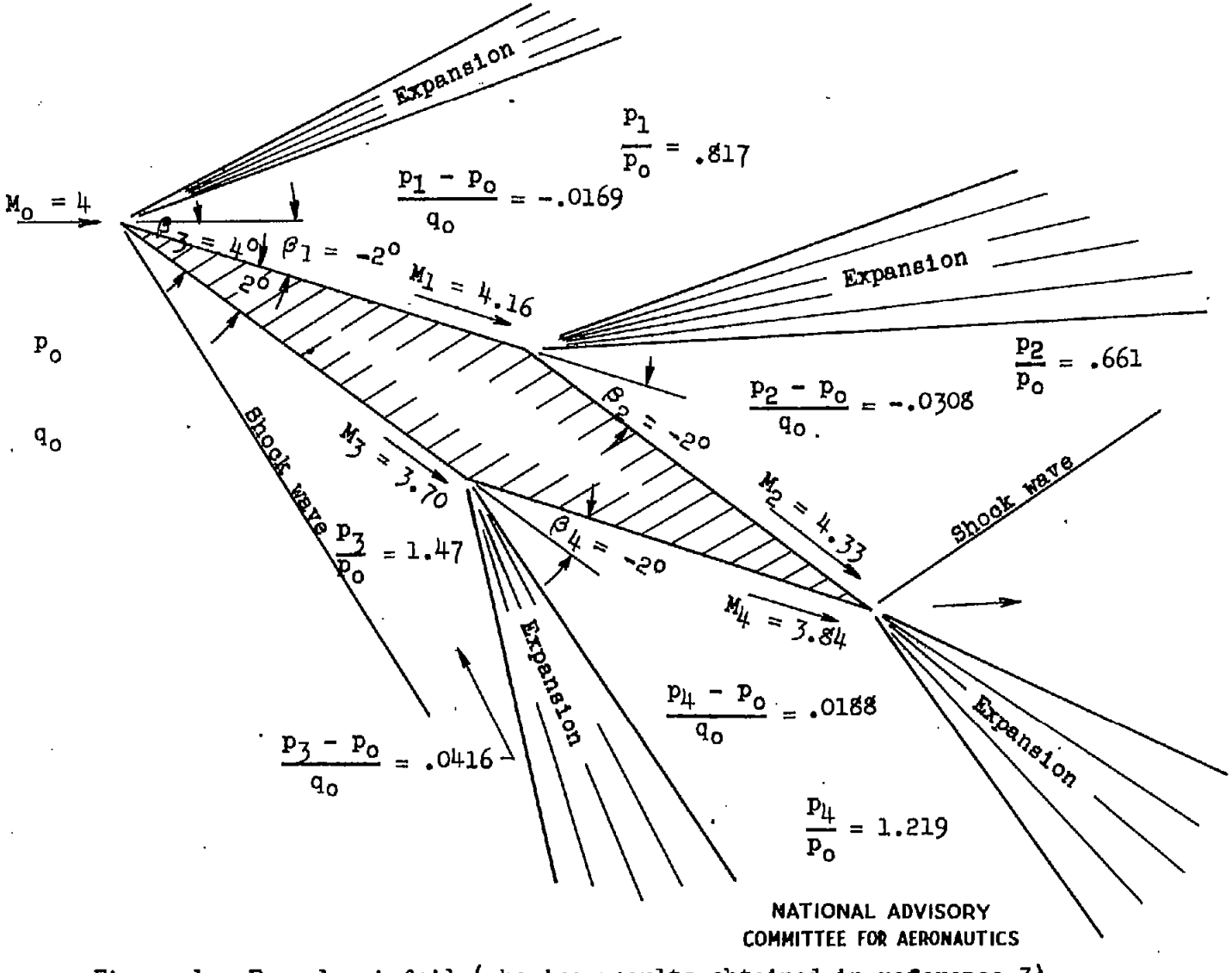

Figure 1.- Example airfoil (showing results obtained in reference 3).

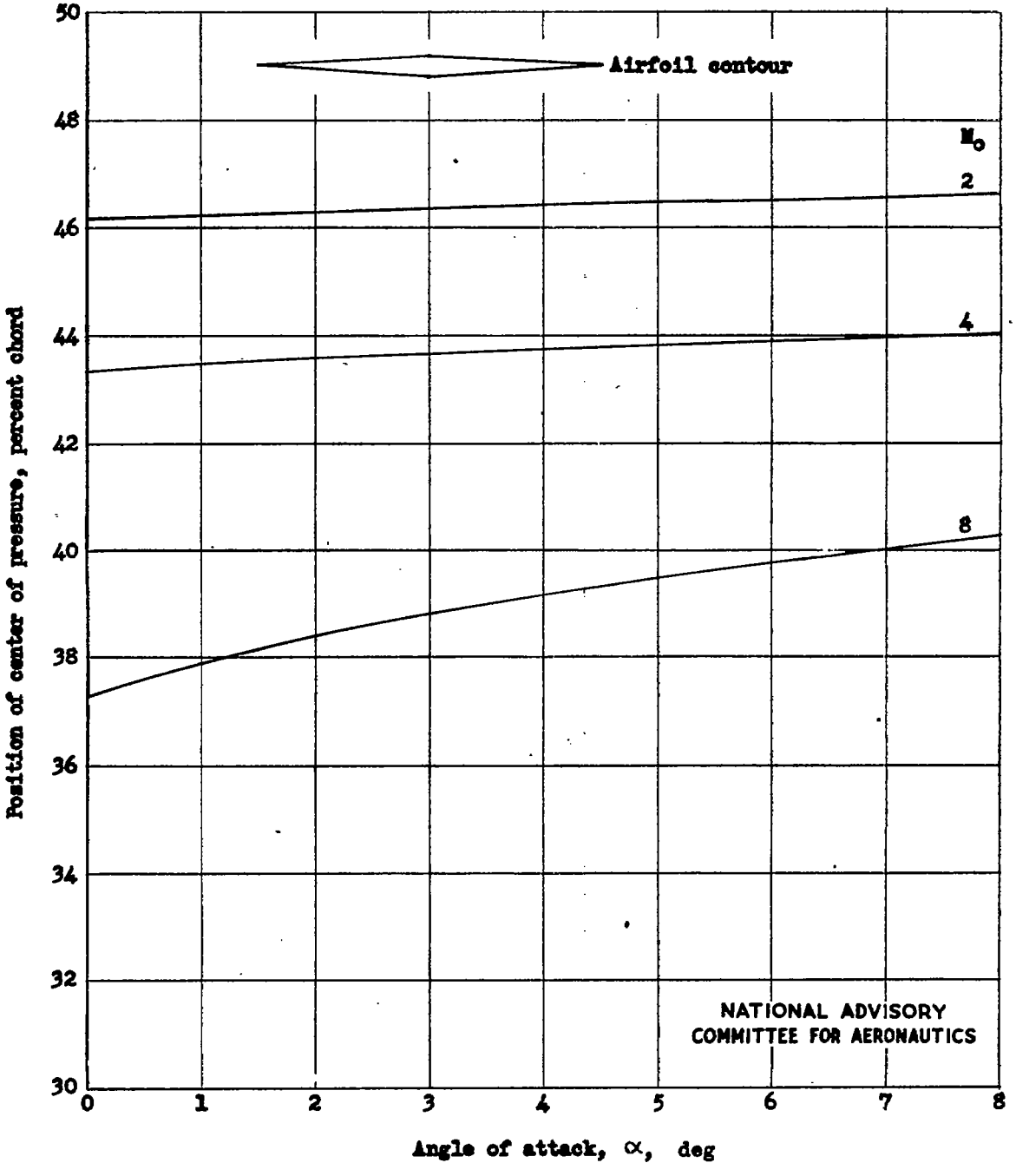

Figure 2.- Position of center of pressure for an uncambered 5- percent-thick airfoil.

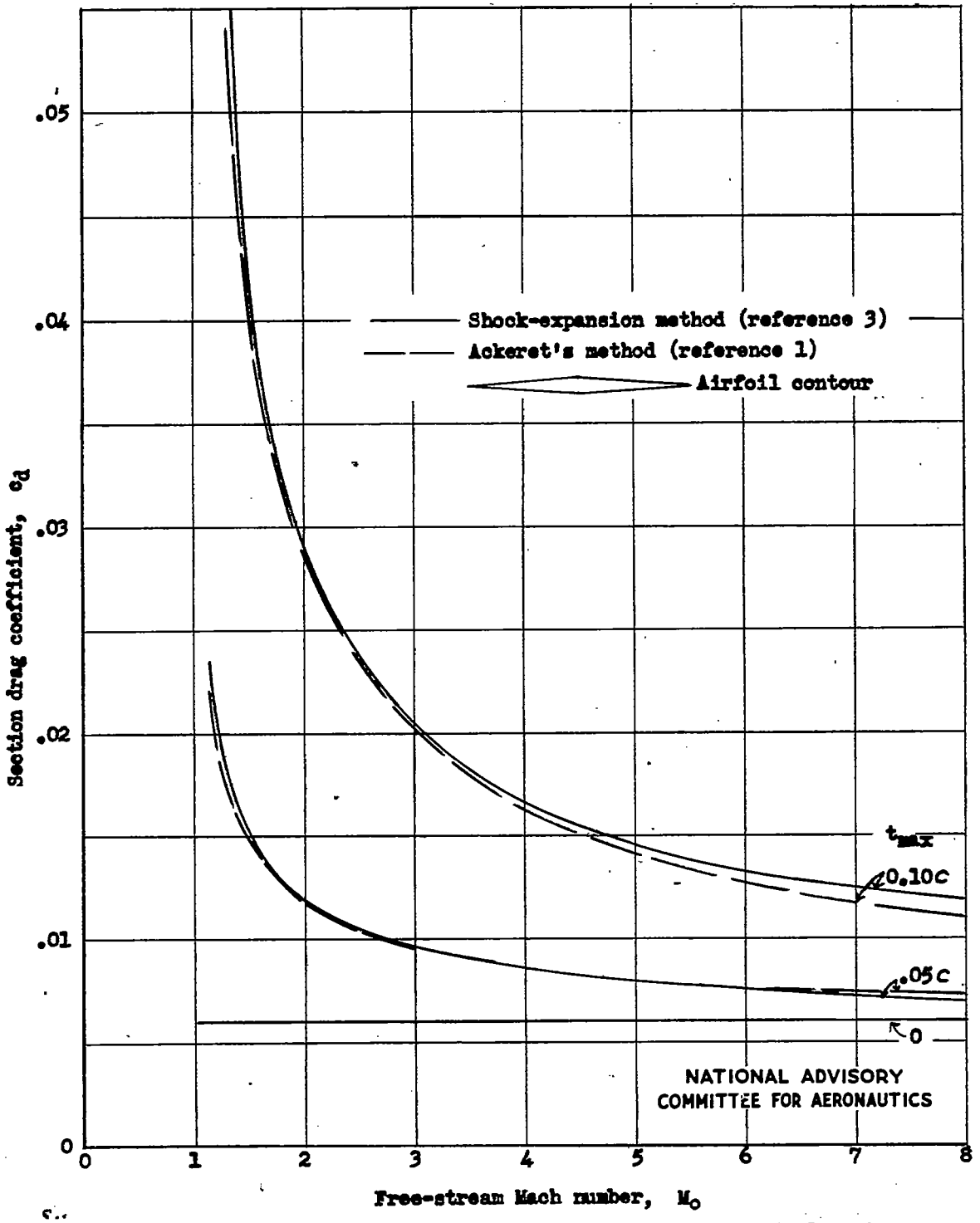

Figure 3.- Drag characteristics of uncambered supersonic airfoils. t_{max} at midchord; $\alpha = 0^o$; $c_l = 0$.

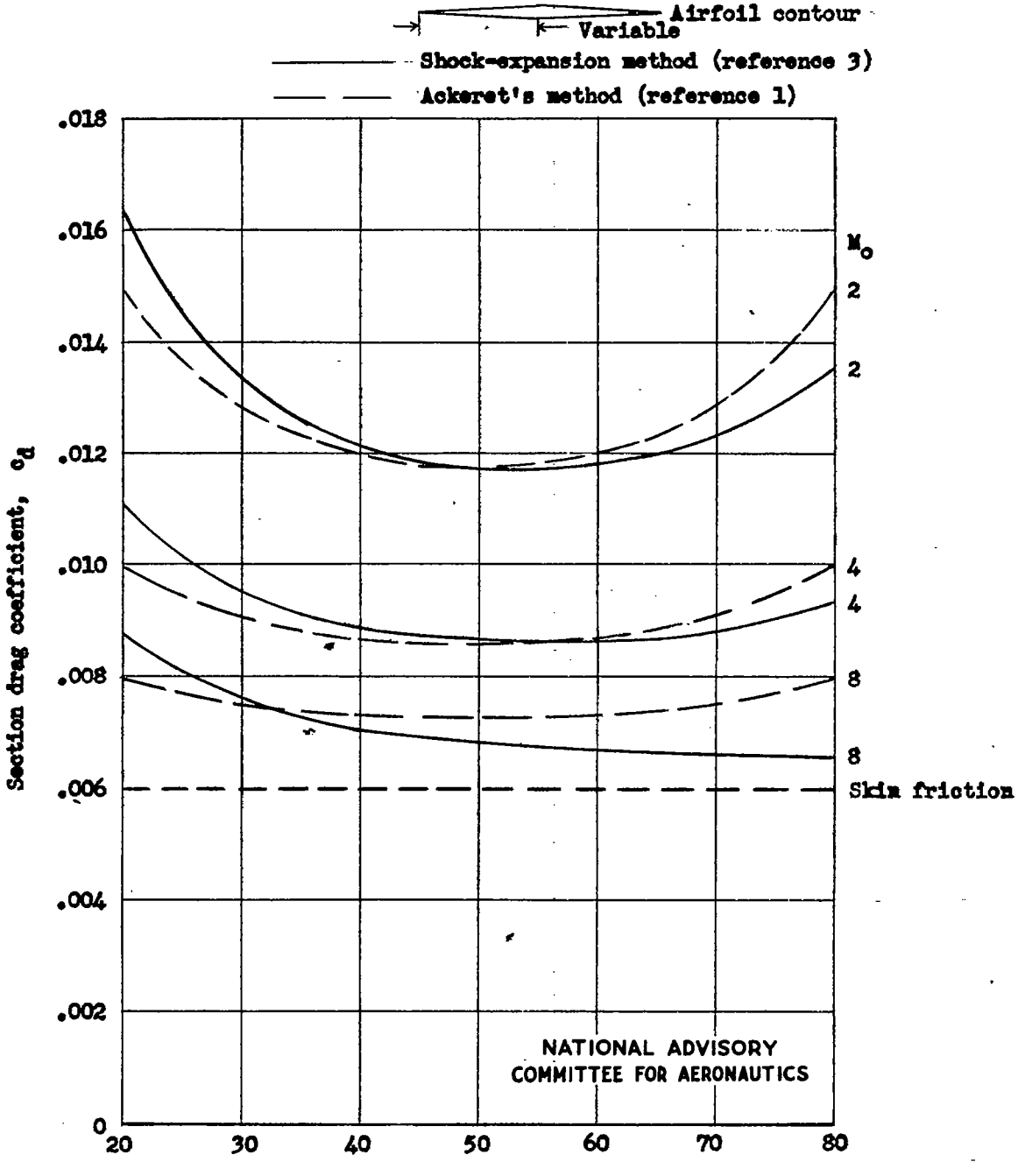

Figure 4.- Effect of location of maximum thickness on drag of 5-percent-thick uncambered airfoil. $\alpha = 0^{\circ}$; $c_l = 0$.

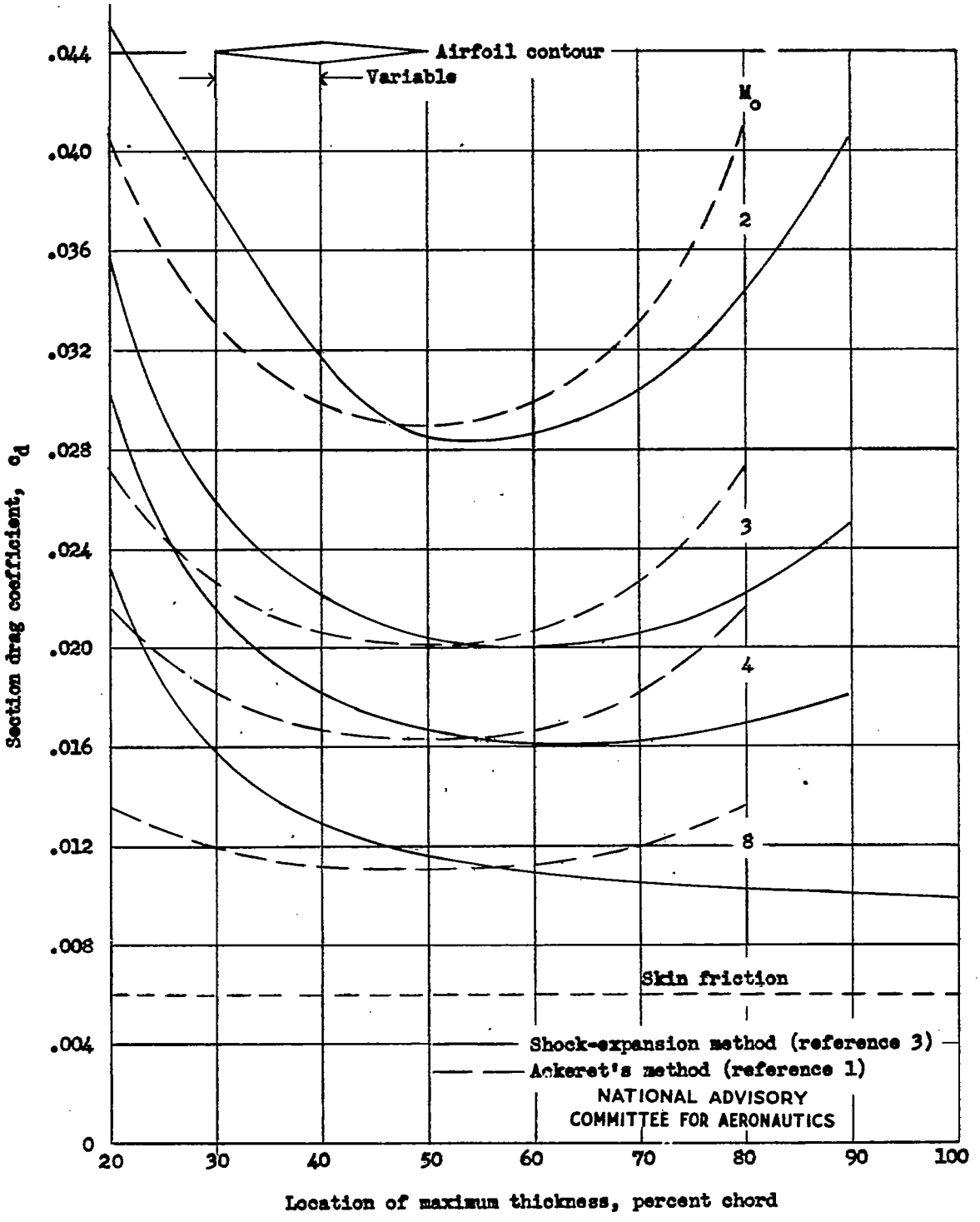

Figure 5.- Effect of location of maximum thickness on drag of 10-percent-thick airfoil.

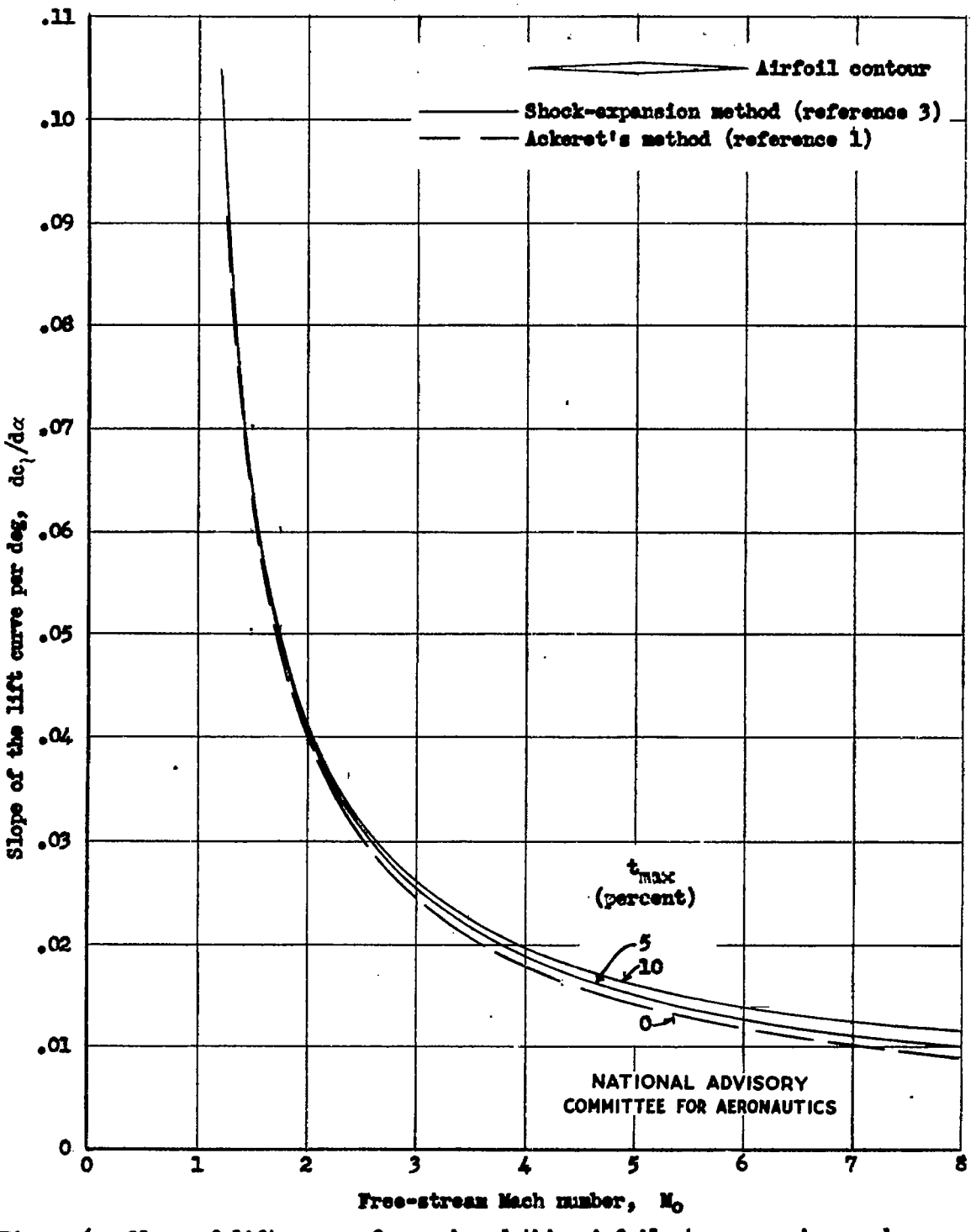

Figure 6.- Slope of lift curve of uncambered thin airfoil at supersonic speeds. t_{max} at midchord; $\alpha = 0°$; $c_l = 0$.

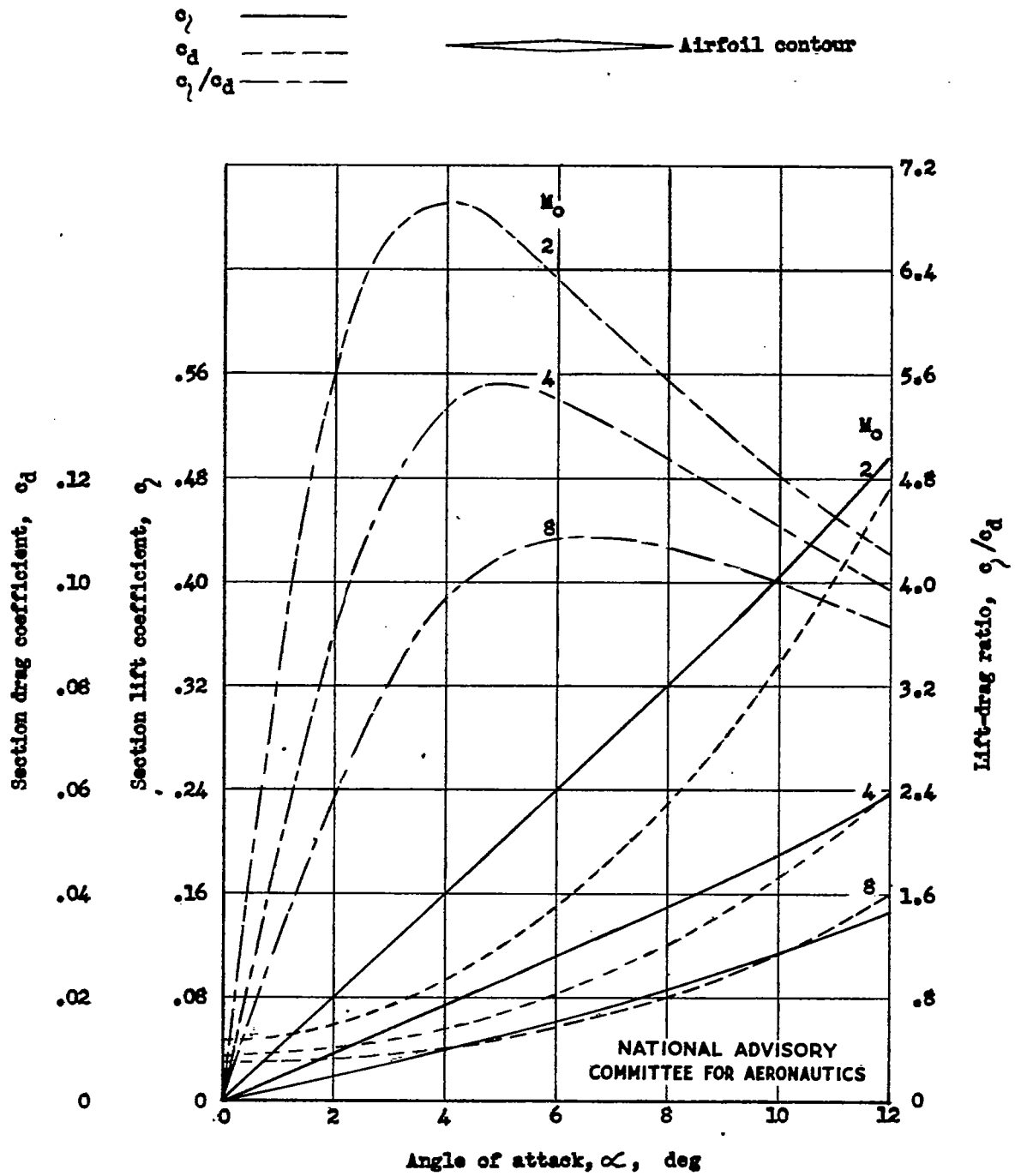

Figure 7.- Effect of angle of attack and Mach number on characteristics of 5-percent-thick uncambered airfoil. t_{max} at midchord; skin friction drag coefficient, 0.0060.

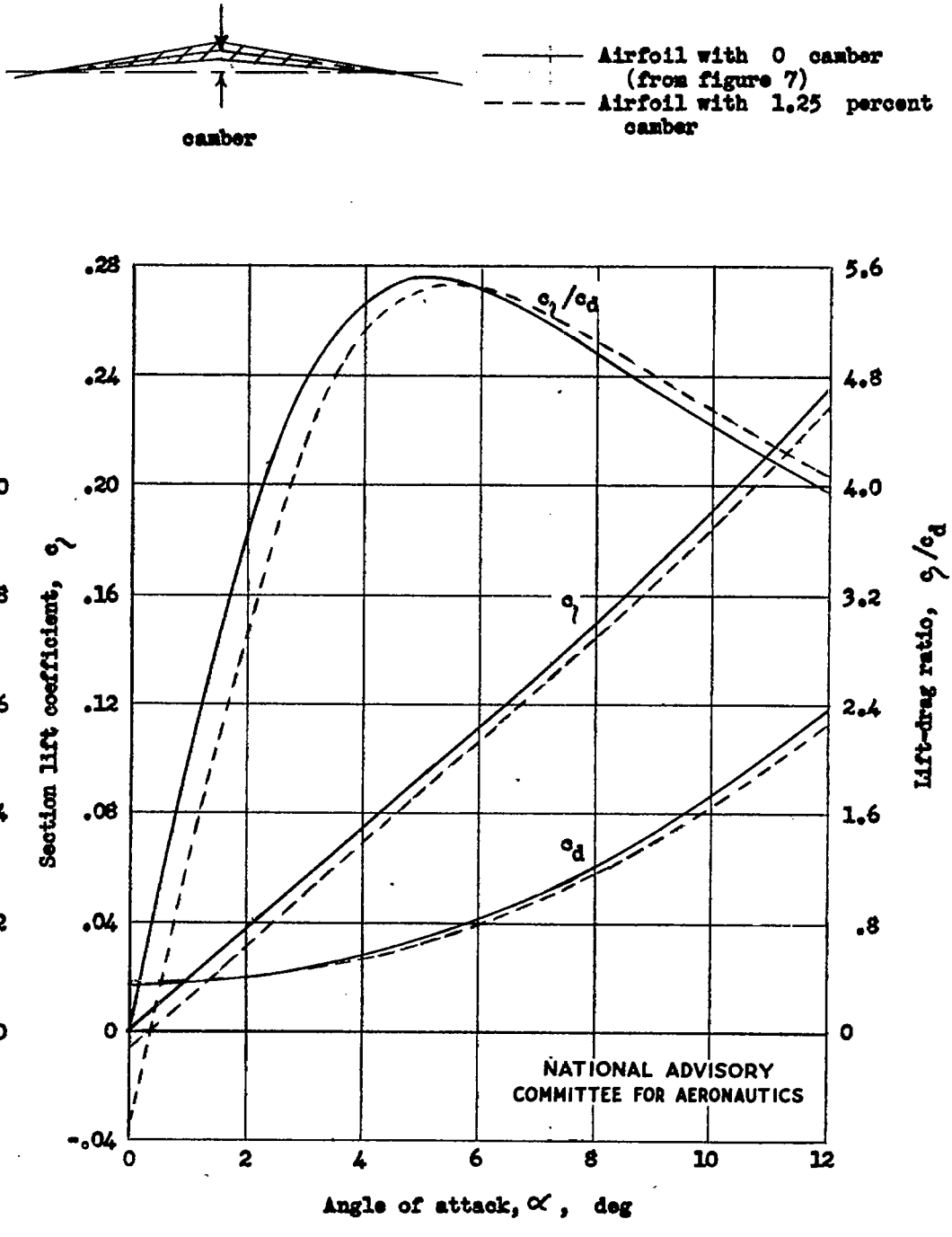

Figure 8.- Effect of angle of attack and camber on characteristics of 5-percent-thick airfoil at $M_0 = 4$.

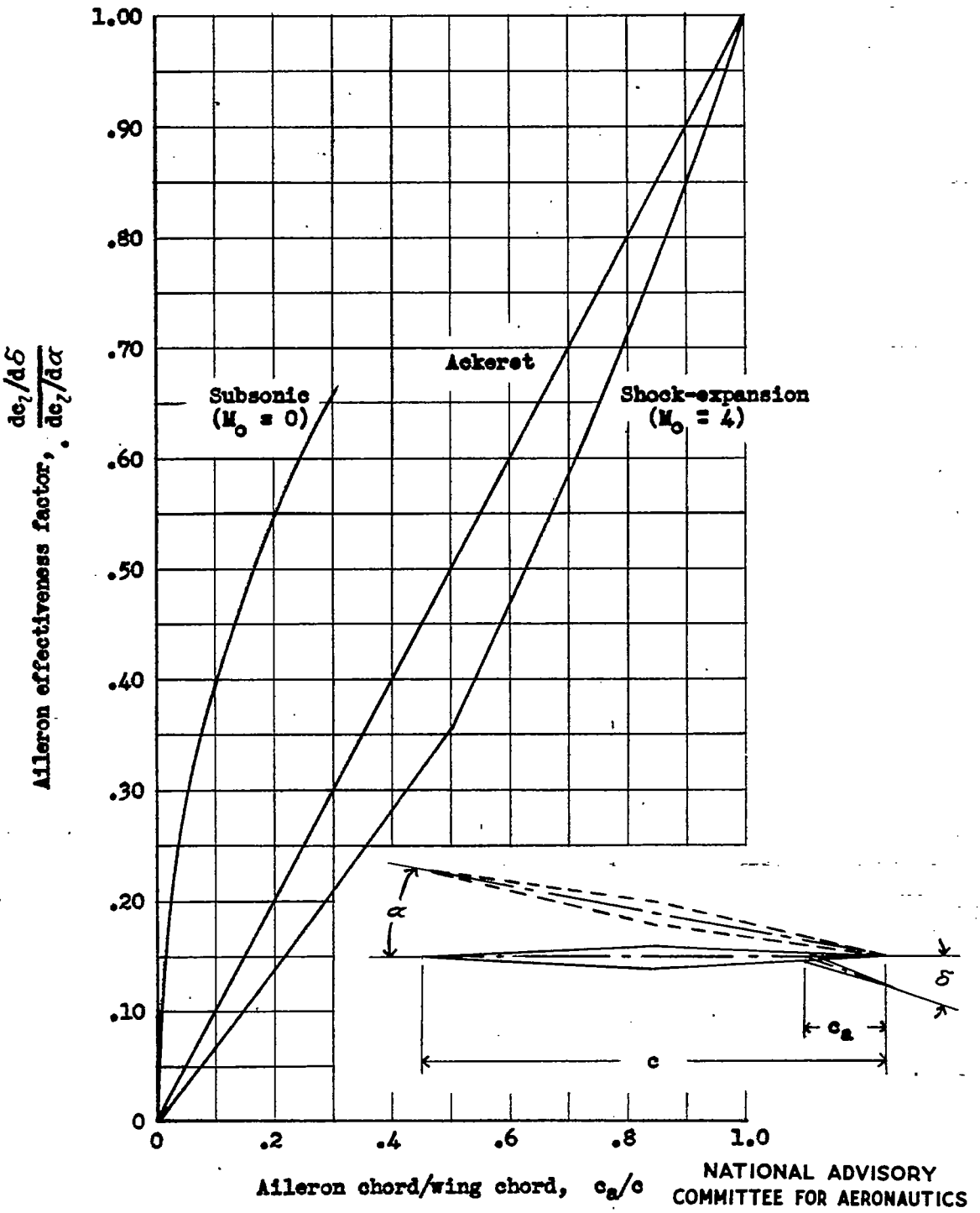

Figure 9.- Aileron effectiveness as a function of the ratio of aileron chord to airfoil chord for 5-percent-thick uncambered airfoil at $M_o = 4$. t_{max} at midchord, 5 percent.

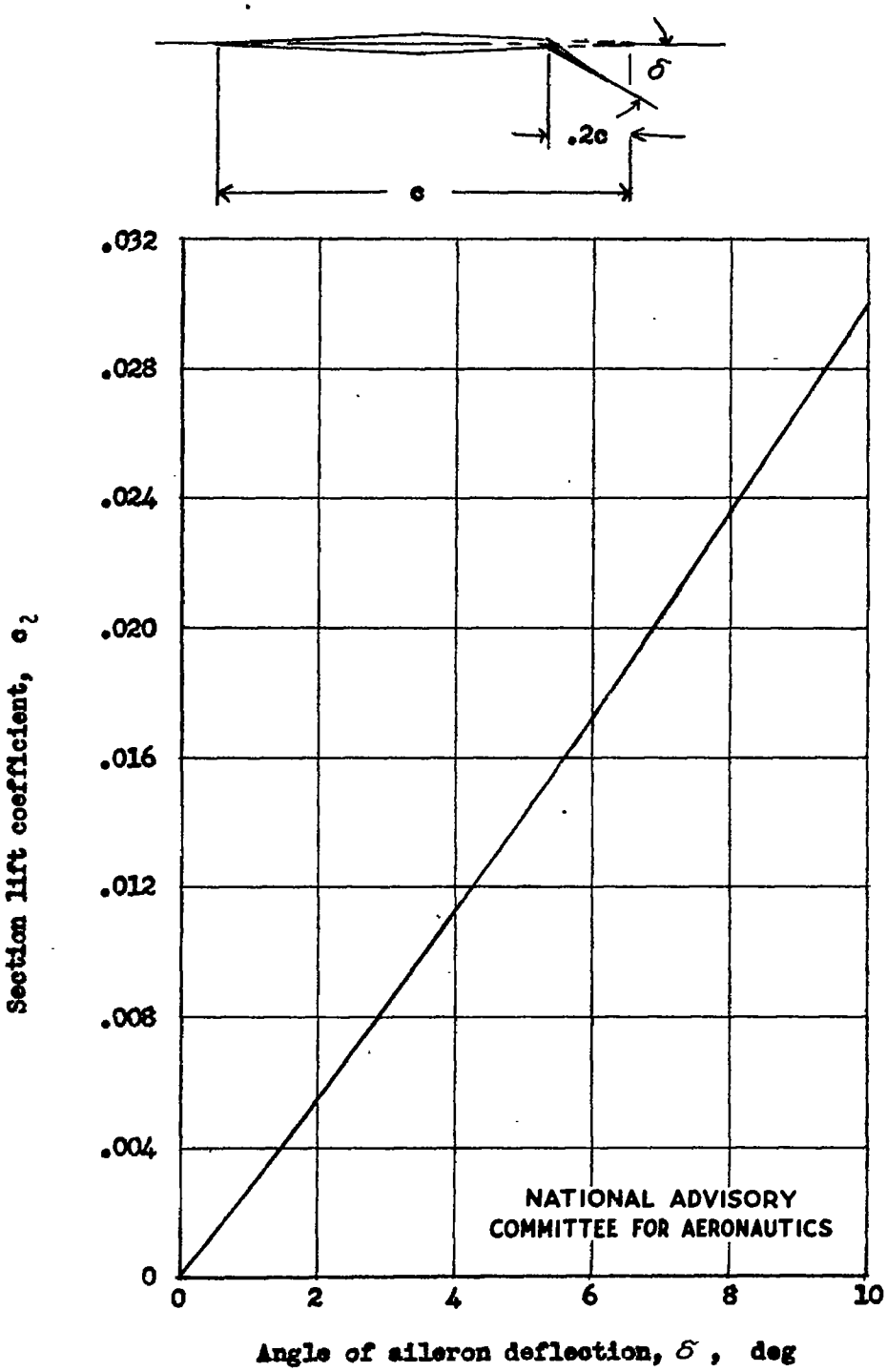

Figure 10.- Variation of airfoil section lift coefficient as a function of aileron deflection for 20 percent chord aileron at $M_0 = 4$. t_{max} at midchord, 5 percent; camber, 0; $\alpha = 0^\circ$.

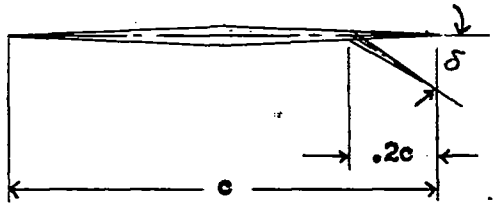

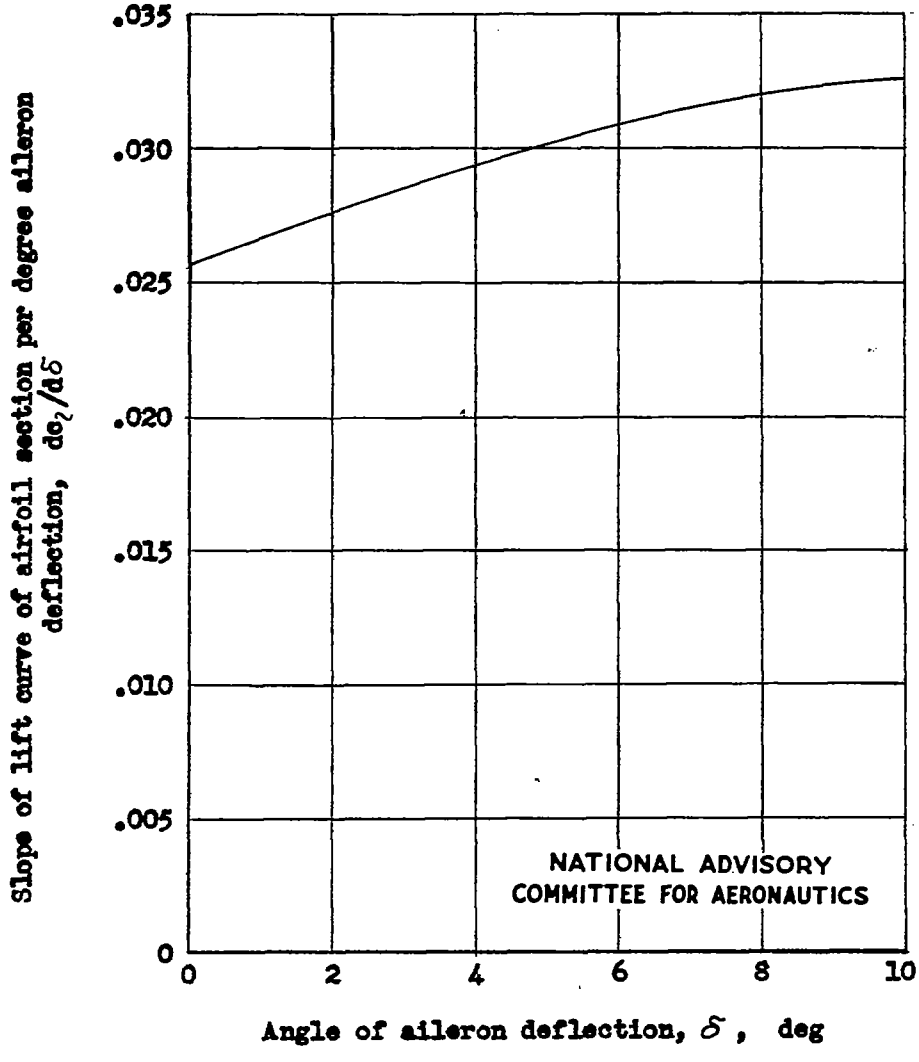

Figure 11.- Slope of lift curve as a function of aileron deflection for 20 percent chord ailerons at $M_0 = 4$. t_{max} at midchord, 5 percent; camber, 0; $\alpha = 0^\circ$.

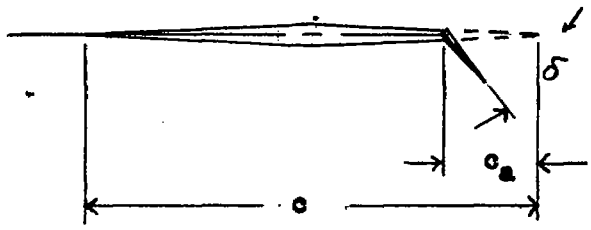

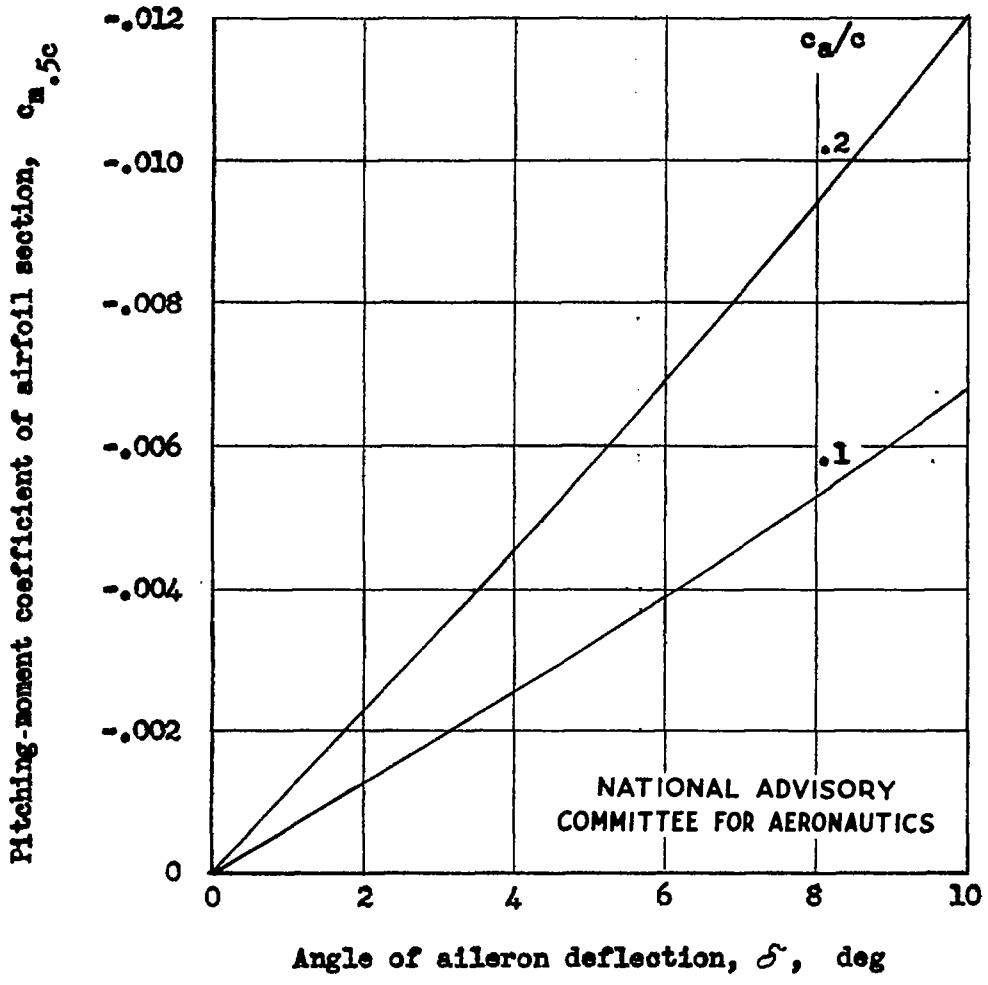

Figure 12.- Effect of aileron deflection on pitching-moment coefficient of airfoil section. t_{max} at midchord, 5 percent; camber, 0; $\alpha = 0^\circ$; $M_o = 4$.

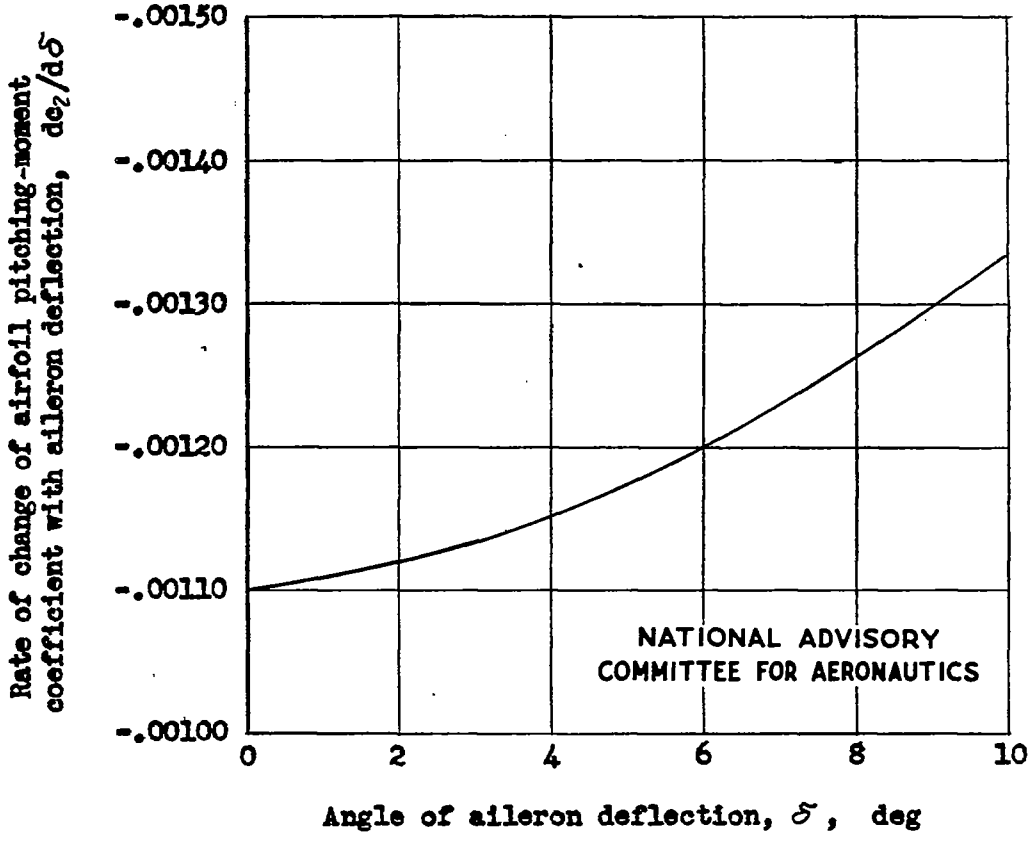

Figure 13.- Effect of aileron deflection on slope of airfoil pitching-moment-coefficient curve for 20 percent chord aileron at $M_0 = 4$. t_{max} at midchord, 5 percent; camber, 0; $\alpha = 0^\circ$.

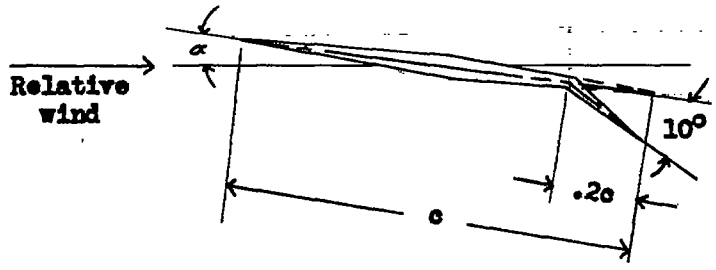

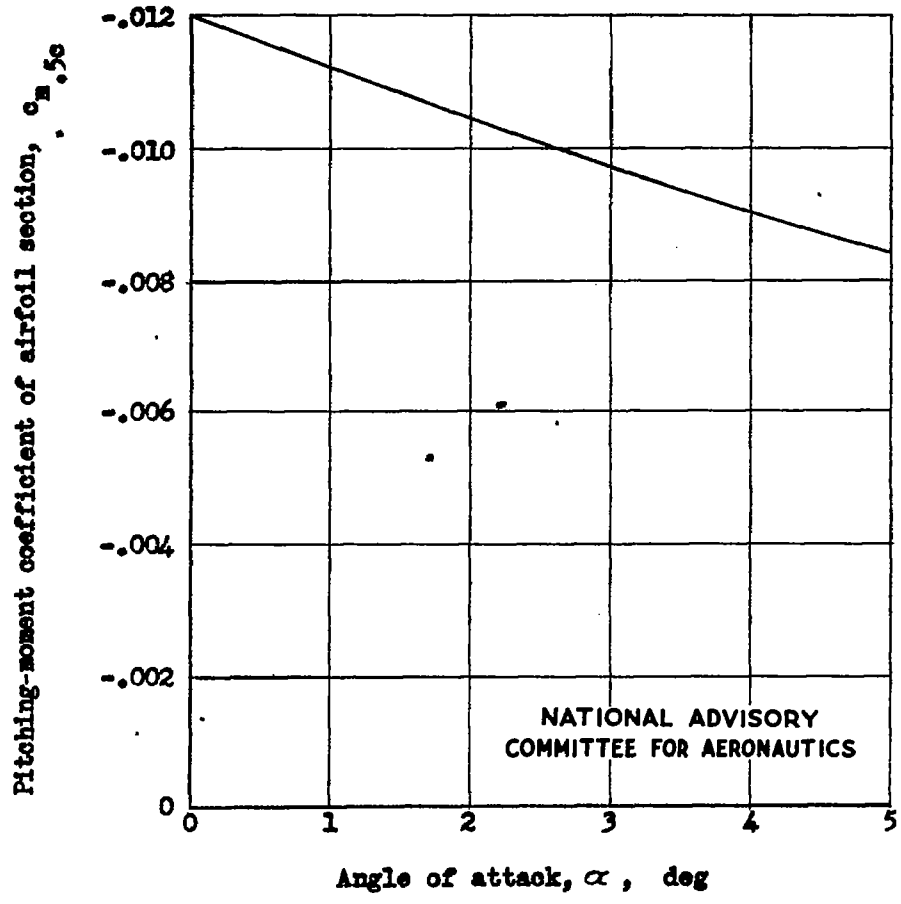

Figure 14.- Effect of angle of attack of airfoil section on section pitching-moment coefficient with 20 percent chord aileron deflected 10° at $M_0 = 4$. t_{max} at midchord, 5 percent; camber, 0.